

# Separation of photonic crystal waveguides modes using femtosecond time-of-flight

M. C. Netti,<sup>a)</sup> C. E. Finlayson, and J. J. Baumberg<sup>a),b)</sup>

*Department of Physics and Astronomy, University of Southampton, Southampton, SO17 1BJ, United Kingdom*

M. D. B. Charlton, M. E. Zoorob, J. S. Wilkinson,<sup>c)</sup> and G. J. Parker

*Mesophotonics Ltd., Chilworth Science Park, Southampton SO16 7NP, United Kingdom*

(Received 10 June 2002; accepted 18 September 2002)

We demonstrate that ultrabroadband ultrashort-pulse white light supercontinua can be used to track the group velocity of photons in optical waveguides using a Kerr gate technique. Results on silicon nitride slab waveguides show both polarization birefringence and multimode dispersion, which vanish at critical wavelengths. When photonic crystals are embedded in the waveguides, the higher order modes are excited within the band-gap region, demonstrating the need to control their dispersion to make effective use of photonic crystal waveguide devices. © 2002 American Institute of Physics. [DOI: 10.1063/1.1520709]

Controlling optical propagation by patterning planar devices in a single microfabrication step makes 2D photonic crystal waveguides extremely attractive for realizing optical integrated circuits. The functionality of the different elements can be engineered by simply modifying the local symmetry and geometry of the photonic crystal (PC) lattice. This corresponds to a modification of the photon dispersion relations and ultimately to a tailoring of group velocity dispersion (GVD), photonic band gaps (PBGs) and localized states. Hence, a whole range of functional elements such as laser cavities,<sup>1–3</sup> channel waveguides,<sup>4–7</sup> bends,<sup>8–10</sup> delay lines,<sup>11</sup> and highly dispersive elements<sup>12</sup> can be integrated on a large scale in a single chip.

In the last few years much effort has been concentrated in taking ideas from modeling these devices into a realizable form.<sup>13</sup> However, experimental evidence for PC optical properties is still a difficult and demanding issue. Measuring the GVD of an optical pulse propagating in a PC device and discriminating its spectral and dynamics features is becoming crucial to the demonstration of useful dispersive properties of PC devices. Several groups have tried to indirectly extract the group velocity dispersion from the phase of Fabry–Perot oscillations between a PC section and sample facets (which are superimposed on emission spectra from their samples).<sup>6,7</sup> However, the direct observation of pulses traveling through PC waveguides remains to be demonstrated.

Previously, we have shown the use of “white light” laser supercontinua for measuring photonic crystal spectral features across very broad wavelength ranges, allowing a detailed match with theoretical models of basic PC properties.<sup>14,15</sup> In this letter we report time-resolved experiments which track ultrashort broadband pulse propagation through 2D photonic crystal waveguides. Optical Kerr

gating<sup>16</sup> is performed on both unpatterned planar and PC waveguides. This allows us to resolve the time-of-flight of photons in each optical mode within the 450–900 nm wavelength region. The different dispersion properties of the propagation of fundamental and higher order modes in a planar waveguide matches a simple model, but does not appear to have been previously presented over such a significant spectral range. The presence of these higher order slab modes together with the PC allows us to clearly discriminate anomalous spectral features in the transmittance spectra which are found inside the photonic band gap.<sup>15</sup> These time-of-flight experiments point to the importance of full characterization of both spectral and temporal modal features for developing integrated optical circuits based on PC technologies.

The samples investigated were silicon nitride waveguides Si<sub>3</sub>N<sub>4</sub> (250 nm nominal thickness,  $n=2.02$ ) embedded in silicon dioxide (SiO<sub>2</sub>) substrate and cladding layer (1.7  $\mu\text{m}$  and 75 nm thick, respectively,  $n=1.46$ ) all grown on silicon. The PC etched slab used here (for test) consists of 40 rows of air holes arranged on a triangular lattice with 260 nm pitch ( $\Lambda$ ) and 150 nm diameter ( $\Phi$ ) (air filling fraction  $f=30\%$ ) and is 10.5  $\mu\text{m}$  long, embedded in the center of waveguide devices  $\sim 1$  cm long, as shown in Fig. 1. An ultrabroadband white light continuum (WLC) from 450 to 1300 nm, which is generated by focusing 1  $\mu\text{J}$  amplified Ti:sapphire pulses in a sapphire crystal, is used as a probe pulse. The transmitted probe pulse emerging from the waveguide is collimated to remove any stray cladding modes contaminating the emission. This pulse is gated by an optical

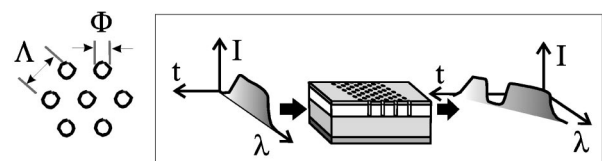


FIG. 1. Sketch of the triangular lattice photonic crystal waveguide used in the experiment. Chromatic dispersion and photonic band-gap effects on a broadband pulse due to the material and photonic crystal are also shown.

<sup>a)</sup>Current address: Mesophotonics Ltd., Chilworth Science Park, Southampton SO16 7NP, UK.

<sup>b)</sup>Electronic mail: j.j.baumberg@soton.ac.uk

<sup>c)</sup>Also with: Electronics and Computer Science, University of Southampton, Southampton SO17 1BJ, UK.

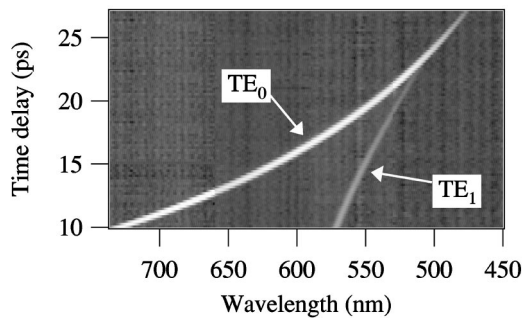


FIG. 2. Image plot of the time-of-flight of the TE polarized white light laser pulse through a 250-nm-thick silicon nitride planar waveguide experimentally measured in the 450–800 nm range. The fundamental ( $TE_0$ ) and higher-order modes ( $TE_1$ ) have a 1000:1 intensity ratio.

Kerr shutter consisting of two crossed polarizers on either side of a 1 mm thick SFL6 glass plate. The optical shutter is opened by focusing a second 1  $\mu$ J regeneratively amplified Ti:sapphire pulse from the same laser (850 nm, 150 fs) onto the same spot on the SFL6 plate which induces a transient birefringence. Due to the high third-order nonlinear susceptibility, this shutter has an almost instantaneous optical Kerr response producing a system time resolution of  $\sim 250$  fs. The advantage of this technique with respect to other nonlinear techniques (such as upconversion and frequency mixing) is the lack of any phase matching requirements in the Kerr shutter, thus allowing a full range of wavelengths and numerical apertures from the waveguide to be analyzed. The gated transmission at each time delay was dispersed by a 1/2 m single spectrometer and detected by a Si CCD. Scanning the time delay of the gate pulse leads to high quality 2D spectra (wavelength versus time):

$$S(\tau, \lambda) = \kappa \int_{-\infty}^{\infty} I_{WG}(t, \lambda) I_{gate}^2(t - \tau) dt,$$

where  $\kappa$  is a constant,  $I_{WG}$  and  $I_{gate}$  are the intensities of the transmitted WLC probe and the gate pulse, respectively. These spectral images in both time and frequency space avoid the errors introduced by measuring the time-of-flight of wavelength-tunable short pulses, which are spectrally reshaped around the band edges.<sup>17</sup> Unlike most measurements in PCs which reconstruct the group velocity from interferometric measurements of the phase shifts (for instance produced by Fabry–Perot fringing in the sample),<sup>18,19</sup> we directly measure the group velocity of the waveguides which is key for practical utilization in communication systems.

To demonstrate the effectiveness of the technique, the 2D image of the time-of-flight of the different spectral components of the WLC is shown in Fig. 2. The propagation delay of the TE mode ( $\mathbf{E} \parallel$  waveguide slab) after traveling through a planar unpatterned waveguide is displayed as a function of the wavelength. Analogous results have been obtained for the TM polarization mode ( $\mathbf{E} \perp$  waveguide slab). The most intense trace is the fundamental mode  $TE_0$ , while the mode emerging between 525 and 575 nm is the first higher-order waveguide mode  $TE_1$ . In order to gain greater insight into the mode dispersions the time-wavelength coordinates are extracted using a Gaussian fit procedure. The time-of-flight of both TE (solid circles) and TM modes (open circles) through the planar silicon nitride waveguides is

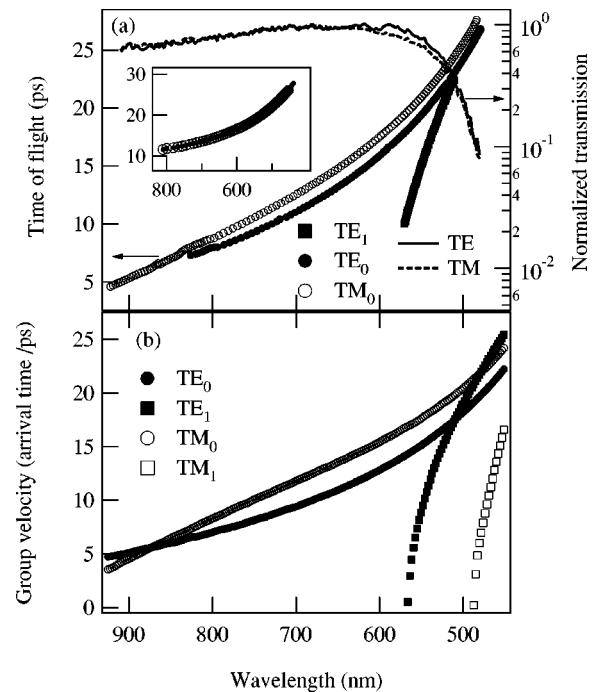


FIG. 3. (a) Time-of-flight spectra of TE (solid symbols) and TM modes (open symbols) through the planar silicon nitride waveguides. Solid and dashed lines are the integrated TE and TM transmittance spectra, respectively. In the inset, the time of flight of the WLC (removing only the sample) is reported for both mode polarizations; (b) calculation of the group velocity of fundamental and higher order TE (solid symbols) and TM (open symbols) modes in a 250-nm-thick slab waveguide, taking into account the normal dispersion of the silicon nitride.

shown in Fig. 3(a), together with their transmittance spectra (solid and dashed line, respectively). For reference, the time of flight of the WLC through the optical system with only the sample removed is shown in the inset for both mode polarizations. This reference scan reveals the expected normal dispersion that the ultrabroadband continuum experiences after traveling through the optics used in the setup, and is identical for TE and TM polarizations. However, when propagating through the unpatterned  $Si_3N_4$  waveguide, the fundamental TE mode travels faster than the TM mode. The modal birefringence typical of slab waveguides is responsible for this polarization-sensitive propagation delay which arises because the TE mode is better confined in the higher refractive index core than the TM mode.<sup>20</sup> Another clear feature is the higher order TE mode (solid squares) which is faster than the fundamental modes near its cutoff. It is excited because the cleaved facets in the polycrystalline waveguide layers lead to some fraction of the input light coupling into the higher order waveguide modes. TM higher order mode cannot be detected in this sample because lies at wavelength shorter than 450 nm.

These results are in good agreement with the calculation of the group velocity of TE and TM modes in a slab waveguide having a 250 nm core thickness which are shown in Fig. 3(b). In this calculation the normal dispersion of the silicon nitride has been taken into account. The cutoff wavelengths of the higher order waveguide modes are proportional to the waveguide thickness, allowing independent non-destructive corroboration of electron microscopy measurements of the thickness of the waveguide. Two further

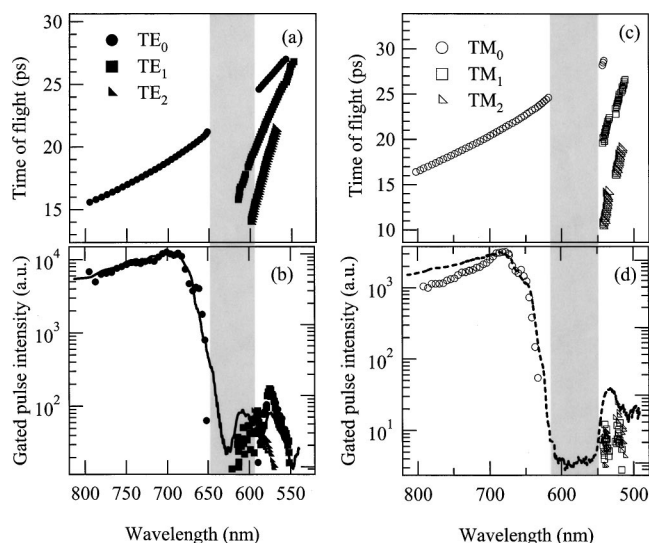


FIG. 4. (a), (c) Time-of-flight spectra for TE- (solid symbols) and TM- (open symbols) polarized white light laser pulses through a rectangular photonic crystal slab ( $f=30\%$ , 40 rows), embedded in the waveguide along the  $\Gamma$ - $J$  direction of propagation; (b), (d) integrated intensities (lines) and time-resolved gated intensities (symbols) for TE and TM polarization modes.

points are of interest: velocity matching occurs for (i) TE and TM fundamental modes at a particular wavelength,  $\lambda_p$  (880 nm) and (ii) for the fundamental and first-order TE modes at a particular wavelength,  $\lambda_m$  (520 nm). Both of these are of potential interest for applications, with (i) allowing polarization-independent waveguide performance, and (ii) allowing phase matching for nonlinear device operation. These results have not been previously apparent because of the lack of such broadband group velocity measurements.

A further advantage of the time-of-flight measurements becomes apparent when the same measurements are taken on waveguides containing rectangular slabs of triangular-symmetry photonic crystal. Time-of-flight spectra for TE- (solid symbols) and TM- (open symbols) polarized white light laser pulses through this PC waveguide along the  $\Gamma$ - $J$  direction of propagation are shown in Figs. 4(a) and 4(c), respectively. In Figs. 4(b) and 4(d) the solid (TE) and dashed (TM) lines record the time-integrated spectral intensities normalized to the input beam spectral intensity (right axis), while, the symbols show the time-resolved gated intensities in each mode (unnormalized, left axis). The most striking feature of these results is the separation of spectral and temporal information carried by the fundamental ( $TE_0, TM_0$ ) and the two higher order modes ( $TE_1, TE_2$  and  $TM_1, TM_2$ ). Both  $TE_0$  and  $TM_0$  modes show photonic band gaps in the 650–590 and 620–550 nm ranges, respectively (shaded areas) which overlap to form a complete PBG between 600 and 620 nm. In contrast to recent reports<sup>7,18</sup> no clear signature of the slowing down of light around the band gap is shown, despite our noise floor being 40 dB below the gated signal. We believe that this is due to scattering and out-of-plane escape of such slow light. However the slope of the group velocity dispersion near the edges of the PBG is anomalous suggesting minor effects blurred by the transform-limited time resolution of our system.

The most striking observation is the presence of higher order modes within the PBG region. Both  $TE_1$  and  $TE_2$  modes exist inside the band gap of the  $TE_0$ , accounting for

the transmittance resonance at 600 nm which reduces the extinction in the gap. The intensities of the gated fundamental and higher order TE and TM reported in Figs. 4(b) and 4(d), respectively, correspond well with the integrated transmission spectra. The intensities of these higher order modes are  $\sim 100$  times weaker than the  $TE_0$  due to the higher losses near their cutoff. TM polarized light is also coupled into  $TM_0, TM_1$  and  $TM_2$  modes but unlike the TE modes, the higher order TM modes do not cross the fundamental mode PBG, explaining the sharp and higher extinction for the TM PBG. Because mode conversion is more efficient for the tighter confined TE polarizations, this clearly shows that higher order modes must be separated from PBGs for effective operation.

In conclusion, we have demonstrated the effectiveness and utility of time-of-flight measurements of ultrabroadband white light continua through nanostructured waveguides for direct determination of group velocity, dispersions, birefringence, and higher order waveguide modes. We find several critical points at which group velocity matching becomes possible between different modes. Correct interpretation of photonic band-gap spectra is shown to be confused by these higher order waveguide modes, and time-of-flight is seen to disentangle these effects. Currently we are extending these measurements across the 350–1800 nm region to allow full characterization of telecom waveguide devices.

- <sup>1</sup>O. Painter, R. K. Lee, A. Scherer, A. Yariv, J. D. O'Brien, P. D. Dapkus, and I. Kim, *Science* **284**, 1819 (1999).
- <sup>2</sup>M. Imada, A. Chiutinan, S. Noda, and M. Mochizuki, *Phys. Rev. B* **65**, 195306 (2002).
- <sup>3</sup>S. Y. Lin, E. Chow, S. G. Johnson, and J. D. Joannopoulos, *Opt. Lett.* **26**, 1903 (2001).
- <sup>4</sup>M. Lončar, D. Nedeljković, T. P. Pearsall, J. Vučković, A. Scherer, S. Kuchinsky, and D. C. Allan, *Appl. Phys. Lett.* **80**, 1689 (2002).
- <sup>5</sup>A. Adibi, Y. Xu, R. K. Lee, A. Yariv, and A. Scherer, *J. Lightwave Technol.* **18**, 1554 (2000).
- <sup>6</sup>X. Letartre, C. Seassal, C. Grillet, P. Rojo-Romeo, P. Viktorovitch, M. Le Vassor d'Yerville, D. Cassagne, and C. Jouanin, *Appl. Phys. Lett.* **79**, 2312 (2001).
- <sup>7</sup>M. Notomi, K. Yamada, A. Shinya, J. Takahashi, C. Takahashi, and I. Yokohama, *Phys. Rev. Lett.* **87**, 253902 (2001).
- <sup>8</sup>A. Mekis, J. C. Chen, I. Kurland, S. Fan, P. R. Villeneuve, and J. D. Joannopoulos, *Phys. Rev. Lett.* **77**, 3787 (1996).
- <sup>9</sup>S. Noda, A. Chiutinan, and M. Imada, *Nature (London)* **407**, 608 (2000).
- <sup>10</sup>Y. Sugimoto, N. Ikeda, N. Carlsson, K. Asakawa, N. Kawai, and K. Inoue, *J. Appl. Phys.* **91**, 3477 (2002).
- <sup>11</sup>S. Lan, S. Nishikawa, H. Ishikawa, and O. Wada, *J. Appl. Phys.* **90**, 4321 (2001).
- <sup>12</sup>H. Kosaka, T. Kawashima, A. Tomita, M. Notomi, T. Tamamura, T. Sato, and S. Kawakami, *Appl. Phys. Lett.* **74**, 1370 (1999).
- <sup>13</sup>M. D. B. Charlton, G. J. Parker, and M. E. Zoorob, *J. Mater. Sci.: Mater. Electron.* **10**, 429 (1999).
- <sup>14</sup>M. E. Zoorob, M. D. B. Charlton, G. J. Parker, J. J. Baumberg, and M. C. Netti, *Nature (London)* **404**, 740 (2000).
- <sup>15</sup>M. C. Netti, M. D. B. Charlton, G. J. Parker, and J. J. Baumberg, *Appl. Phys. Lett.* **76**, 991 (2000).
- <sup>16</sup>S. Kinoshita, H. Ozawa, Y. Kanematsu, I. Tanaka, N. Sugimoto, and S. Fujiwara, *Rev. Sci. Instrum.* **71**, 3317 (2000); J. Takeda, K. Nakajima, S. Kurita, S. Tomimoto, S. Saito, and T. Suemoto, *Phys. Rev. B* **62**, 10083 (2000).
- <sup>17</sup>K. Inoue, N. Kawai, Y. Sugimoto, N. Carlsson, N. Ikeda, and K. Asakawa, *Phys. Rev. B* **65**, 121308 (2002).
- <sup>18</sup>H. Kitahara, N. Tsumura, H. Kondo, M. W. Takeda, J. W. Haus, Z. Yuan, N. Kawai, K. Sakoda, and K. Iou, *Phys. Rev. B* **64**, 045202 (2001).
- <sup>19</sup>A. Inhof, W. L. Vos, R. Sprik, and A. Lagendijk, *Phys. Rev. Lett.* **83**, 2942 (1999).
- <sup>20</sup>K. Okamoto, *Fundamentals of Optical Waveguides* (Academic, New York, 2000).